Influence of ENSO and the Atlantic Multidecadal Oscillation on Drought over the United States

KINGTSE C. MO, JAE-KYUNG E. SCHEMM, AND SOO-HYUN YOO

Climate Prediction Center/NCEP/NWS, Camp Springs, Maryland

(Manuscript received 8 December 2008, in final form 19 June 2009)

ABSTRACT

Composites based on observations and model outputs from the Climate Variability and Predictability (CLIVAR) drought experiments were used to examine the impact of El Niño–Southern Oscillation (ENSO) and the Atlantic multidecadal oscillation (AMO) on drought over the United States. Because drought implies persistent dryness, the 6-month standardized precipitation index, standardized runoff index, and soil moisture anomalies are used to represent drought. The experiments were performed by forcing an AGCM with prescribed sea surface temperature anomalies (SSTAs) superimposed on the monthly mean SST climatology. Four model outputs from the NCEP Global Forecast System (GFS), NASA's Seasonal-to-Interannual Prediction Project, version 1 (NSIPP1), GFDL's global atmospheric model, version 2.1 (AM2.1), and the Lamont-Doherty Earth Observatory (LDEO)/NCAR Community Climate System Model, version 3 (CCM3) were analyzed in this study. Each run lasts from 36 to 51 yr.

The impact of ENSO on drought over the United States is concentrated over the Southwest, the Great Plains, and the lower Colorado River basin, with cold (warm) ENSO events favoring drought (wet spells). Over the East Coast and the Southeast, the impact of ENSO is small because the precipitation responses to ENSO are opposite in sign for winter and summer. For these areas, a prolonged ENSO does not always favor either drought or wet spells.

The direct influence of the AMO on drought is small. The major influence of the AMO is to modulate the impact of ENSO on drought. The influence is large when the SSTAs in the tropical Pacific and in the North Atlantic are opposite in phase. A cold (warm) event in a positive (negative) AMO phase amplifies the impact of the cold (warm) ENSO on drought. The ENSO influence on drought is much weaker when the SSTAs in the tropical Pacific and in the North Atlantic are in phase.

1. Introduction

Long-lasting drought has an enormous impact on the nation's economy and society. Skillful drought prediction can mitigate devastating economic effects on people and ecosystems. To improve drought forecasts, one needs to understand the causes that trigger and sustain drought. Because drought implies prolonged rainfall and soil moisture deficits, they are often modulated by low-frequency sea surface temperature anomalies (SSTAs). In the Pacific, decadal trends of SSTAs in the North Pacific and the tropical Pacific can influence the drought occurrence over the United States (Mo and Schemm 2008a; Dai et al. 2004; Goodrich 2007; Hidalgo and Dracup 2003). In the interannual frequency band, ENSO has a large influence on the occurrence of-drought (Ropelewski and Halpert 1986, 1989; Dai et al. 1998; Mo and Schemm 2008a). Barlow et al. (2001) attributed both the North Pacific SSTAs and ENSO as major causes for summer droughts over the United States.

In the Atlantic, the Atlantic multidecadal oscillation (AMO) mode has been linked to rainfall and river flow anomalies over the United States. The AMO is defined as the first rotated empirical orthogonal function (EOF) of non-ENSO SSTAs, but the associated principal component (PC) is highly correlated to the mean Atlantic SSTAs from the equator to 60°N (Mestas-Nunez and Enfield 1999). The warm (cold) phase of the AMO is associated with less (more) rainfall over the Mississippi River basin and more (less) streamflow over Lake Okeechobee in Florida (Enfield et al. 2001). McCabe

Corresponding author address: Kingtse C. Mo, Climate Prediction Center/NCEP/NWS/NOAA, 5200 Auth Rd., Camp Springs, MD 20746.
E-mail: kingtse.mo@noaa.gov

DOI: 10.1175/2009JCLI2966.1

et al. (2004) correlated 20-yr moving drought frequency with 20-yr AMO time series. They found that the warm (cold) phase of the AMO is associated with increased (decreased) drought occurrence over the Southwest and the north-central United States, and fewer (more) drought events over Florida. While ENSO has been identified as the major driver of severe droughts and persistent wet spells over the United States, many studies concluded that the Atlantic SSTAs play a secondary role to sustaining drought (Schubert et al. 2004; Seager et al. 2005; Seager 2007).

In addition to the direct influence of the AMO on drought, the AMO can modulate the influence of ENSO on drought. For example, Enfield et al. (2001) found that the ENSO impact on winter rainfall depends on the phase of the AMO. Rogers and Coleman (2003) found that interactions between the AMO and the Pacific teleconnection modes modulate the Mississippi streamflow in winter. Different phases of the AMO also link to different summer precipitation modes of the North American monsoon (Hu and Feng 2008).

With the progress of climate modeling, current climate models in general are able to predict ENSO relatively well (Saha et al. 2006). Responses to SSTAs in the Atlantic simulated by atmospheric GCMs (AGCMs) are more diverse. In the review paper by Kushnir et al. (2002), the authors stated that the atmosphere indeed responds to the SSTAs in the Atlantic. However, the response is small in comparison to natural unforced variability (Kushnir and Held 1996). Both thermal heating and eddy feedback contribute to the response. The response also depends on the strength of SSTAs and the model's climate state (Peng et al. 1995).

Over the United States, the observed precipitation (P) and SST data cover less than 150 yr. These datasets do not cover enough AMO cycles to produce robust statistics for diagnostic studies. From the observations, it is difficult to separate decadal trends and ENSO. Trends are not linear and results may depend on the method used to isolate trends. One possibility is to rely on AGCM experiments to confirm observational findings. The AGCM experiments designed by the U.S. Climate Variability and Predictability (CLIVAR) drought working group (Schubert et al. 2009) are well suited for this purpose. The drawback of model experiments is that models have errors. Not all model errors can be reduced by correcting the model's climatology. Therefore, both observations and model experiments are needed to study the extreme precipitation events and atmospheric responses to the low-frequency SSTA forcing.

The purpose of this paper is to examine the impact of (i) ENSO, (ii) the AMO, and (iii) the combinations of the different phases of the AMO and ENSO on drought and wet spells over the United States. We draw our conclusions from composites based on observations and model simulations from the U.S. CLIVAR experiments. The observational datasets and a brief description of the U.S. CLIVAR experiments are outlined in section 2. The influence of ENSO on drought is discussed in section 3. The impact of the decadal AMO on drought is presented in section 4, and the indirect influence of the AMO on drought through ENSO is given in section 5. Physical mechanisms are examined based on model outputs. Conclusions and discussions are given in section 6.

2. Data and experiments

a. Data

There are many types of droughts (Keyantash and Dracup 2002): Meteorological drought is related to P deficits, soil moisture deficits are used to identify agricultural drought, and hydrological drought is represented by a shortage of either streamflow or runoff. Many cooperative observation stations are available from 1900 to the present (Wang et al. 2009), but long-term observational soil moisture and runoff are scarce. Therefore, soil moisture and runoff were obtained from the North American Land Data Assimilation System (NLDAS). The longest data available were obtained from the Variable Infiltration Capacity (VIC) model from the University of Washington. The dataset covers the period from 1915 to 2006. The horizontal resolution is 0.5°. The model has three soil layers, with the top layer fixed at 10 cm and the other two layers at variable depths. The same dataset was used by Andreadis et al. (2005) to study drought. The detailed documentation of the VIC model can be found on the University of Washington Web site (available at http://www.hydro.washington.edu/forecast/monitor).

The P forcing for the VIC model is based on the cooperative observer station meteorological daily data with the Precipitation Regression on Independent Slopes Method (PRISM) correction (Maurer et al. 2002). We use the P data from the VIC for this study to ensure that P, soil moisture, and runoff are consistent. The differences between the monthly mean P anomalies from this dataset and from the Climate Prediction Center (CPC) unified gauge-based P analysis (Higgins et al. 2000) for the overlapping period of 1950–2006 are small. The daily maximum and minimum temperature and low-level winds used to force the VIC model were taken from the National Climatic Data Center (NCDC) archive of cooperative observer station meteorological daily data (Maurer et al. 2002).

Because drought means persistent water deficits, we use the 6-month standardized precipitation index (SPI6)

to measure the P deficit or wetness (Hayes et al. 1999; McKee et al. 1993, 1995). To calculate SPI6 for the current month's temperature (T), the 6-month P mean from month $T - 5$ to T was obtained. The distribution of the time series of 6-month P means was transformed from a gamma distribution function to a normal distribution. SPI6 at T was determined according to the normal distribution. SPI6 will identify drought lasting more than one season.

We use the 6-month standardized runoff index (SRI6) to measure the runoff deficits. The computation of SRI6 is the same as that of the SPI6 except runoff is used instead of precipitation (Shukla and Wood 2008; Mo 2008). The total water storage [soil moisture (SM)] is used to measure agricultural drought. The characteristic time for soil moisture anomalies is about 6–12 months over the eastern United States and about 24–36 months over the western region (Mo and Schemm 2008b). SPI6, SRI6, and soil moisture have comparable characteristic times. They are used as indices to study drought.

The drought classification is based on the same criterion as the drought monitor (Svoboda et al. 2002). A drought event is defined as when the SPI6 or SRI6 index is less than -0.8 or when the soil moisture percentile is less than 20% (Svoboda et al. 2002). A wet spell is defined as the opposite extreme, that is, when the SPI6 or SRI6 index is greater than 0.8 or the SM percentile is greater than 80%. For the CLIVAR model runs, there is internal consistency between the soil moisture, runoff, and P. Not all models archive runoff and soil moisture. Therefore, SPI6 was used as the index to study drought.

The SST data are the monthly reconstructed SSTs from Smith et al. (1996) updated to 2006. The dataset covers the base period of 1915–2006. The horizontal resolution is 2°. Climatological monthly means for the base period are removed from each dataset to obtain anomalies.

The rotated empirical orthogonal function (REOF) analysis was performed on the annual mean global SSTAs to obtain the leading SST modes (Schubert et al. 2009). The detailed procedures and discussions are provided online (see http://gmao.gsfc.nasa.gov/research/clivar_drought_wg/index.html). The first mode represents the global trends. The second mode is the Pacific SST mode representing ENSO (Fig. 1a). It shows positive SSTAs extending from the central to the eastern Pacific, with negative SSTAs in the North and South Pacific. The AMO is represented by the third mode of the annual mean SSTAs or first mode of the SSTAs over the Atlantic (Fig. 1b). It shows a horseshoe-shaped pattern with positive SSTAs over the North Atlantic from 60° to 75°N and over the tropical North Atlantic. This mode resembles the first non-ENSO mode (Mestas-Nunez and Enfield 1999). The decadal variations of the associated PC resemble the AMO. According to Enfield et al. (2001), Hu and Feng (2008), and McCabe et al. (2004), the warm phase of the AMO covered the periods of 1930–59 and 1995–2006, while the cold phase covered the periods of 1915–25 and 1965–90.

Composites are used to study the influence of ENSO and the AMO on drought over the United States. The seasonal mean SSTAs for winter [January–March (JFM)], spring [April–June (AMJ)], summer [July–September (JAS)], and autumn [October–December (OND)] were projected onto the REOF 2 (Fig. 1a) or REOF 3 (Fig. 1b) to obtain the rotated principal component (RPC). Warm (cold) events were selected when RPC was great than 1 (less than -1) standard deviation. Composites of P, SPI6, SRI6, and SM anomalies were obtained for positive and negative RPC events separately. The results are displayed as the differences between cold and warm events. To study the impact of the combinations of the two modes, composites were computed for the positive and negative ENSO events for the warm AMO phase (1930–59 and 1995–2006) and the cold AMO phase (1915–25 and 1965–90) separately.

To test the statistical significance of a composite map from observations or the frequency of the drought occurrence from a model experiment, the Monte Carlo method was used (Mo and Schemm 2008b). We use the P composite as an example to describe the method. Composites were computed from randomly selected maps from the same P time series. The process was repeated 500 times. The statistical significance of the tested map can be determined from these 500 cases at each grid point. The anomaly composite should be within 5% of the distribution function determined by the composites of the randomly selected maps. The areas in which the values of the composite field are statistically significant at the 5% level are shaded (or colored). The composites of SPI6 or the frequency of drought occurrence can also be tested the same way.

b. U.S. CLIVAR SST experiments

The GCM experiments were designed by the U.S. CLIVAR drought working group to study the relationships between persistent SST forcing and drought (information online at http://gmao.gsfc.nasa.gov/research/clivar_drought_wg/index.html).

The AGCM is forced by prescribed SST boundary conditions in combinations of the Pacific (P) mode (Fig. 1a) and the Atlantic (A) mode (Fig. 1b). Positive or negative anomalies associated with the warm (w) phase or the cold (c) phase of each pattern were added to the SST monthly mean climatology to form a global SST distribution to force the AGCM (Schubert et al. 2009).

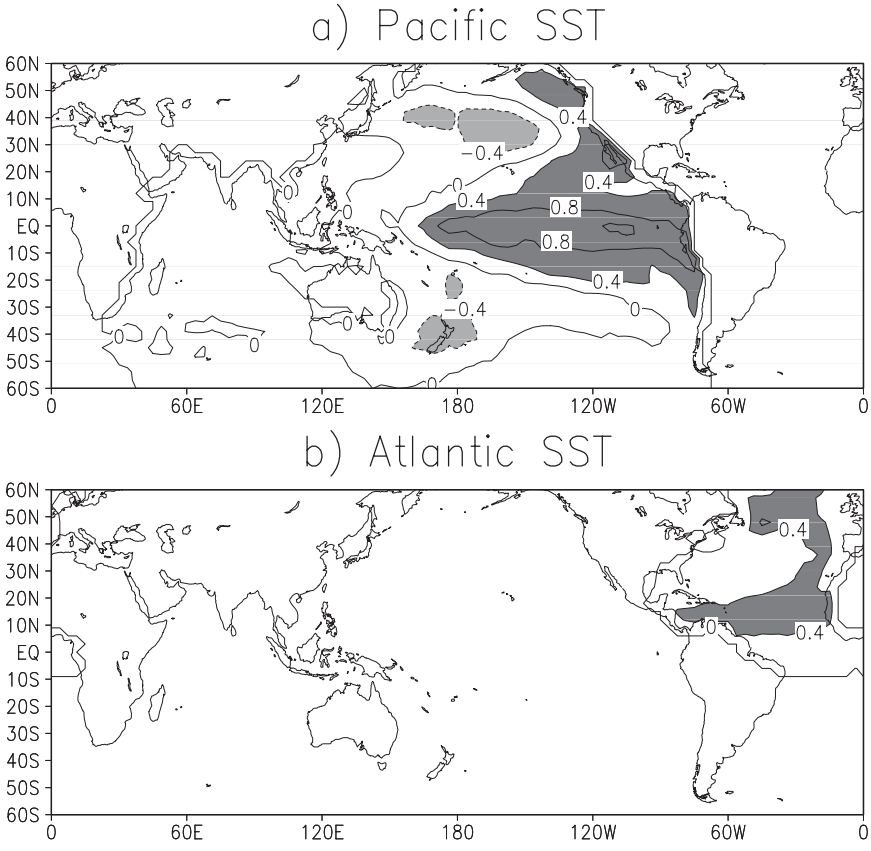

FIG. 1. The (a) Pacific and (b) Atlantic SSTA patterns. Contour interval is 0.4 nondimensional units. Positive anomalies are shaded.

The same forcing repeats each year. Therefore, trends are not included. The experiment forced by the monthly mean climatology is labeled as PnAn. The experiments with the combinations of the Pacific or/and the Atlantic anomalies (Fig. 1) are labeled as PxAy, where x is labeled as c for cold, w for warm, and n for neutral SSTAs in the Pacific. Similarly, y denotes the SSTAs in the Atlantic. For example, the experiment that is forced by cold (warm) SSTAs in the Pacific but that has no SST anomalies in the Atlantic is labeled PcAn (PwAn); the experiment that is forced by warm SSTAs in the Atlantic and cold anomalies in the Pacific is labeled PcAw.

We analyzed nine experiments: PnAn, PwAn, PcAn, PnAw, PnAc, PcAc, PcAw, PwAc, and PwAw from the National Centers for Environmental Prediction (NCEP) Global Forecast System (GFS; Campana and Caplan 2005), National Aeronautics and Space Administration's (NASA's) Seasonal-to-Interannual Prediction Project, version 1 (NSIPP1; Bacmeister et al. 2000; Schubert et al. 2004), Geophysical Fluid Dynamics Laboratory (GFDL) global atmospheric model, version 2.1 (AM2.1; Delworth et al. 2006; Milly and Shmakin 2002), and the Lamont-Doherty Earth Observatory (LDEO)/National Center for Atmospheric Research (NCAR) Community Climate Model, version 3 (CCM3; Kiehl et al. 1998; Seager et al. 2005). They are labeled as the GFS, NSIPP, GFDL, and CCM3 experiments, respectively. Each GFS experiment lasts only 36 yr. The NSIPP and the GFDL experiments last for 50 yr, and the CCM3 experiments last for 51 yr. From each run P and 200-hPa height and 200-hPa wind monthly means were extracted. For the GFS runs, the vertically integrated moisture flux (qflux) and flux divergence $D(Q)$ were derived from cross products (qu and qv) at all levels.

The GFS is used as an example to describe the procedures used to calculate the frequency of drought occurrence and anomalies. We pooled P from nine experiments together to form a time series of $36 \times 12 \times 9$ months. The total SSTAs averaged over the nine experiments are zero. To determine the impact of SSTAs on drought, we calculated the drought occurrence of the pooled time series. The 6-month SPI6 was calculated from the pooled time series of monthly mean anomalies. The first year of each experiment was discarded. For each experiment, the frequency of drought occurrence

was determined by counting the number of months (num) that the SPI6 is below −0.8 at each grid point. Because each experiment has a different length of integration, the frequency of occurrence is given as the ratio between num and the total length of the experiment. For the GFS, the length is 35×12. The statistical significance is assessed by the Monte Carlo method. The model reaches its climatological state after 5 yr of integration, so the persistence is naturally taken into consideration. If we shuffle the years in the pooled series, we mimic the SSTA variation in nature. The frequency of occurrence is still the same. Of course, reality is not so simple. For example, there are more SSTA modes than ENSO and the Atlantic mode.

For each experiment, the ensemble mean of any variable was obtained by taking the equally weighted mean of that variable from the GFS, NSIPP, CCM3, and GFDL model runs. The climatological monthly means (grand means) can be calculated each month from this pooled time series. They are similar to the climatological monthly means calculated from the PnAn experiment. For each experiment, the monthly mean anomaly is defined as the departure from the grand monthly mean or the climatological mean from the PnAn experiment for that month.

3. Impact of ENSO on drought over the United States

a. Observations

Composite differences of *P* and SPI6 between positive and negative events were obtained for each season based on RPC associated with Fig. 1a (Fig. 2). There is no filter applied to RPC. If the ENSO warm and cold events were selected according to the Niño-3.4 index, the results were similar. The *P* responses to ENSO are seasonally and regionally dependent (Figs. 2e–h). The responses to a cold ENSO winter are negative *P* anomalies over the southern United States, California, the Great Plains, the Southeast, and the East Coast from Florida to 40°N, and positive *P* anomalies over the Pacific Northwest and the Ohio Valley. The signal for spring is weak. For JAS, a cold ENSO event is likely associated with positive *P* anomalies over the East Coast and the Southeast, and negative anomalies over the north-central United States. For OND, negative anomalies are located over the Southwest and the Eastern United States east of 100°W, excluding the Northeast. Positive anomalies are located over the Pacific Northwest. The cold (warm) ENSO events favor dryness (wetness) for the Southwest and the Great Plains for all seasons. If a cold (warm) ENSO event persists for many seasons, dry (wet) conditions over these regions are likely to persist. The situation is very different for the East Coast and the Southeast where the *P* responses to ENSO for winter and summer are opposite in phase. For these regions, a persistent ENSO does not always favor persistent drought or wet spells (Mo and Schemm 2008b).

This point can be illustrated by the SPI6 composites that measure the occurrence of persistent drought or wet spells (Figs. 2a–d). The SPI6 for JFM is contributed by *P* anomalies from OND and JFM. It shows that drought is more likely to occur over the Southeast, the Southwest, and the Great Plains, and wet spells are like to occur over the Pacific Northwest during cold ENSO events. The composite for AMJ is similar to that of JFM. The composite for JAS is weak. The OND composite shows dryness over New Mexico, the Colorado basin, the southern plains, and the north-central United States. For warm ENSO events, the situation reverses.

In addition to SPI6, soil moisture and runoff indices are used to represent hydrological and agricultural droughts (Mo 2008). The composites of soil moisture anomalies and SRI6 were obtained the same way as the SPI6 composite (Fig. 3). The composite of each index was computed for each season separately based on RPC2. Then, we averaged over four seasons. The composites based on different indices are consistent. They show that a cold (warm) ENSO favors drought (wetness) over the Great Plains and the Southwest. In contrast, there is no strong signal over the East Coast and the Southeast. The seasonal cycles of *P* for these regions are weak (Mo and Schemm 2008a). Therefore, *P* anomalies for many seasons can contribute to long-term measures of drought, such as SPI6. The *P* responses to ENSO are opposite in phase for winter and summer and an ENSO event often lasts more than two seasons. These are reasons for weak signal over the East Coast and the Southeast. The large differences between *P* and SPI6 composites illustrate that drought means persistent *P* deficits.

b. Model experiments

The frequency of drought occurrence is presented as the percentage of number of months that SPI6 < -0.8 for a given experiment. To examine the influence of ENSO on drought, we present the frequency of drought occurrence for the PwAn (i.e., a warm Pacific with no Atlantic forcing) and PcAn (i.e., a cold Pacific with no Atlantic forcing) experiments for each model and for the multimodel ensembles averaged over four models (Fig. 4). Because the monthly mean SST anomalies repeat each year, there is no decadal signal. This is one way to separate impacts from decadal trends and ENSO on drought.

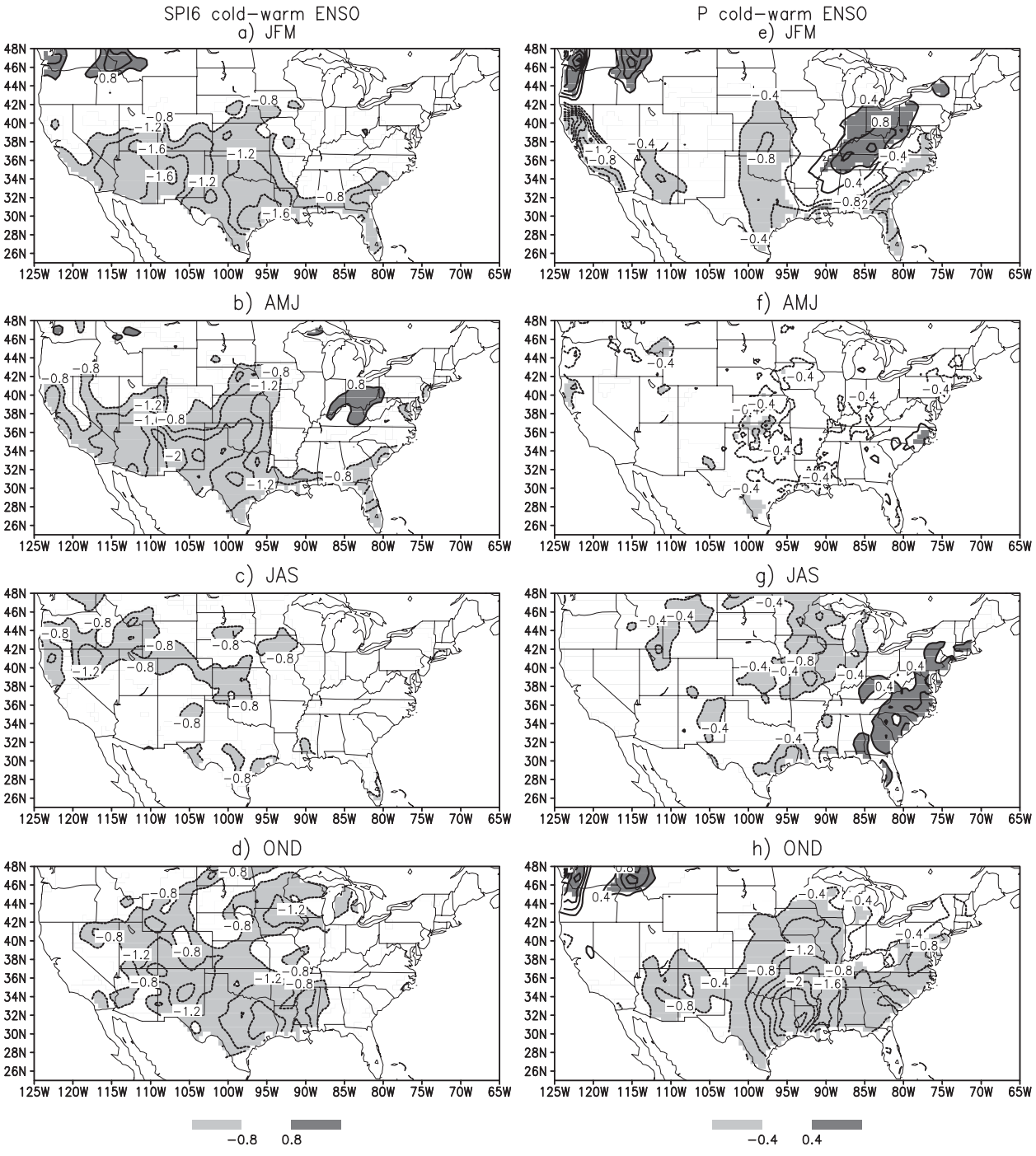

FIG. 2. Composite difference of SPI6 between cold and warm ENSO events for (a) JFM, (b) AMJ, (c) JAS, and OND. SPI6 was derived from *P* analysis. Contour interval is 0.4, with values between −0.8 and 0.8 omitted. Areas where positive (negative) differences are statistically significant at the 5% level based on the Monte Carlo test are shaded dark (light). (e)–(h) As in (a)–(d), but for *P*. Contour interval is 0.4 mm day^{-1}.

The multimodel ensemble means are consistent with the composites based on observations (Fig. 3). The cold Pacific SSTAs (PcAn) favor more drought events (Fig. 4e) over the Southwest, the lower Colorado River basin, and the Great Plains, with a minimum over Texas. ENSO has very little influence on drought over the Southeast and the East Coast. PwAn has the opposite impact.

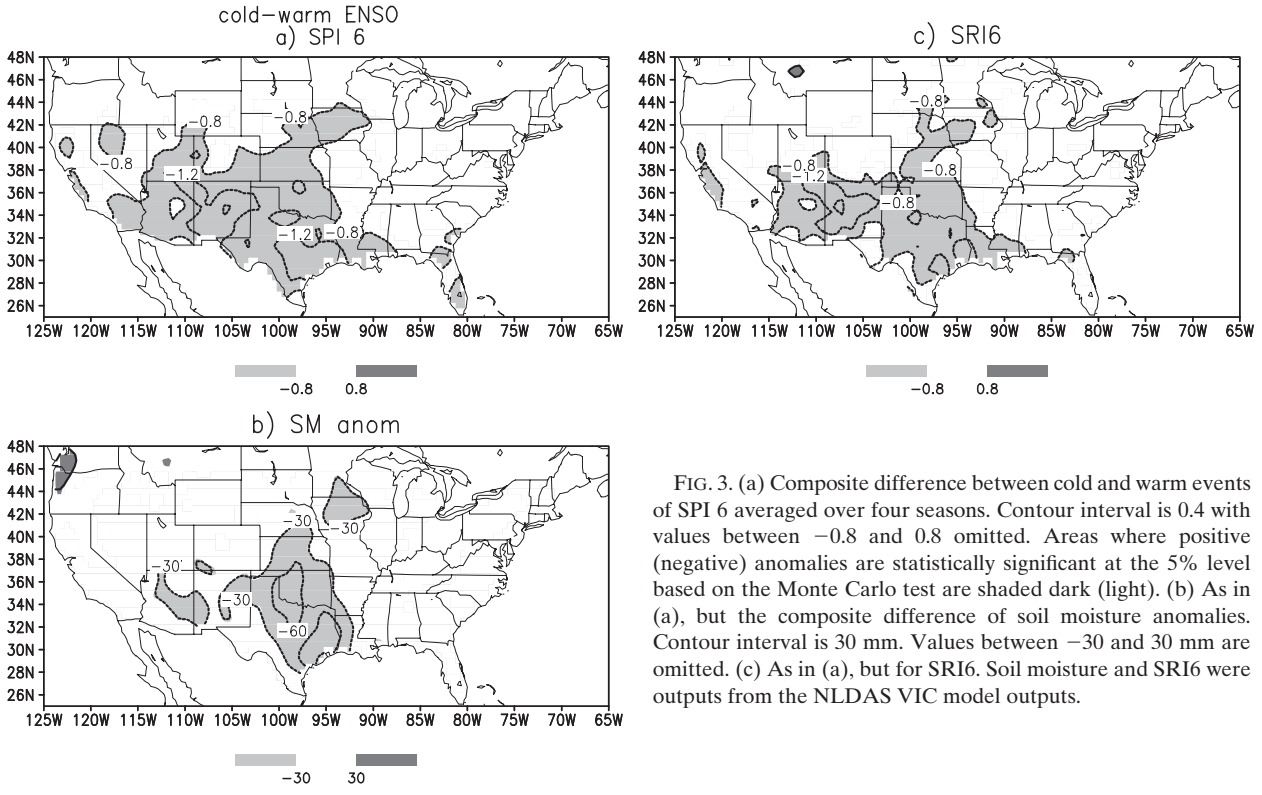

FIG. 3. (a) Composite difference between cold and warm events of SPI 6 averaged over four seasons. Contour interval is 0.4 with values between −0.8 and 0.8 omitted. Areas where positive (negative) anomalies are statistically significant at the 5% level based on the Monte Carlo test are shaded dark (light). (b) As in (a), but the composite difference of soil moisture anomalies. Contour interval is 30 mm. Values between −30 and 30 mm are omitted. (c) As in (a), but for SRI6. Soil moisture and SRI6 were outputs from the NLDAS VIC model outputs.

While the multimodel ensemble compares favorably with the ENSO composites from the observations (Fig. 3), there are large variations from one model to another. The GFS, NSIPP, and GFDL capture the west–east contrast, but they differ in spatial patterns (Fig. 4). The GFDL model shows the impact of ENSO extending to 85°W while the impact is limited to the west of 90°W for the GFS model runs. The NSIPP runs show that the largest impact of a perpetual ENSO is located over the central United States and the Southwest. The CCM3 runs show that the influence of ENSO extends to the East Coast and weakens signals over the Colorado River basin. While the models still have large errors they compensate for one another, and the multimodel ensemble has the most reliable results.

To examine the evolution of the model runs, we plotted the time series of *P* averaged over the Great Plains (32°–40°N, 90°–105°W) and the Southeast (26°–32°N, 75°–87°W land points) for winter (December–March, red line), summer (June–September, green line), and the entire year (dark crosses) for each model (Fig. 5). The *P* averaged over the Great Plains (Figs. 5a–h) settles into the model's climatology after a period of spinup. All models show positive anomalies for the PwAn experiment and negative anomalies for the PcAn experiment. The *P* responses over the Great Plains are not seasonally dependent. For the GFS, CCM3, and GFDL runs, both summer and winter *P* anomalies contribute to drought (wet spells). The NSIPP runs show large responses in summer and almost no response in winter.

For the Southeast (Figs. 5i–p), the situation is very different. The GFS and GFDL models capture the phase reversal between the winter and summer responses to ENSO so that the net responses are small. The NSIPP model has no response in winter; the contributions come entirely from summer rainfall. The CCM3 model captures the phase reversal between summer and winter, but the response for winter is stronger than that for summer so that the annual response to PwAn (PcAn) is positive (negative).

To show the *P* response to ENSO over the United States, the *P* climatological seasonal means averaged over the last 25-yr of a given experiment are calculated to avoid spinup. Figure 6 shows the *P* mean differences between the PwAn and PcAn experiments. Both the GFS and the GFDL runs capture the ENSO influence on *P* reasonably well, in comparison with the observations (Fig. 2). However, the GFS model misses the negative *P* anomalies over the Pacific Northwest and the GFDL model does not capture the negative *P* anomalies over the Ohio Valley in winter. Both models miss negative anomalies over the East Coast in summer. The NSIPP runs have no response over the United States in winter and summer anomalies over the Great Plains are

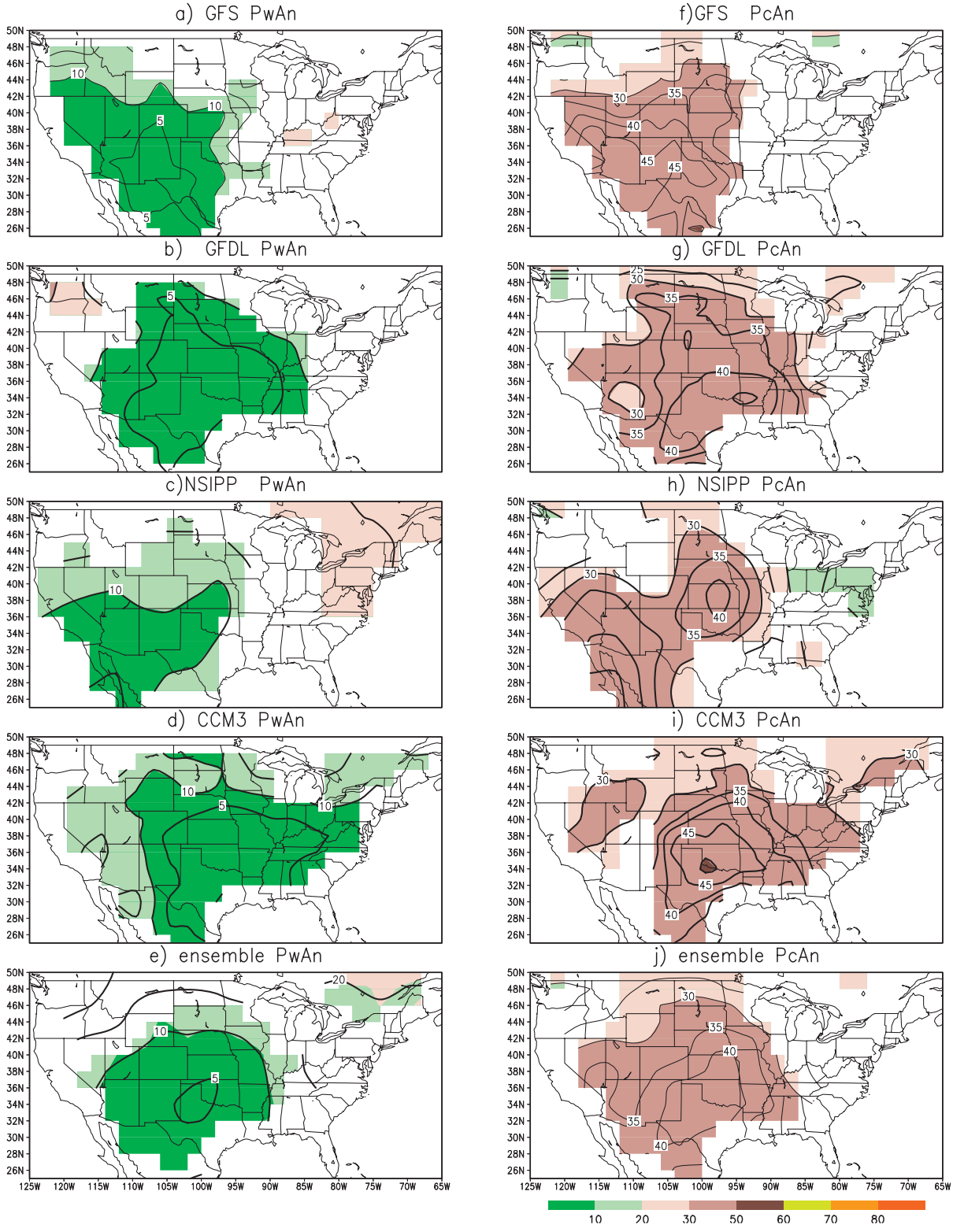

FIG. 4. The frequency of drought occurrence × 100 for the (a) GFS, (b) GFDL, (c) NSIPP, and (d) CCM3 PwAn experiment, and (e) ensemble mean of the four models for the PwAn experiment. Contour interval is 5. Areas where values are statistically significant at the 5% level based on the Monte Carlo test are colored. (f)–(j) As in (a)–(e), but for the PcAn experiments.

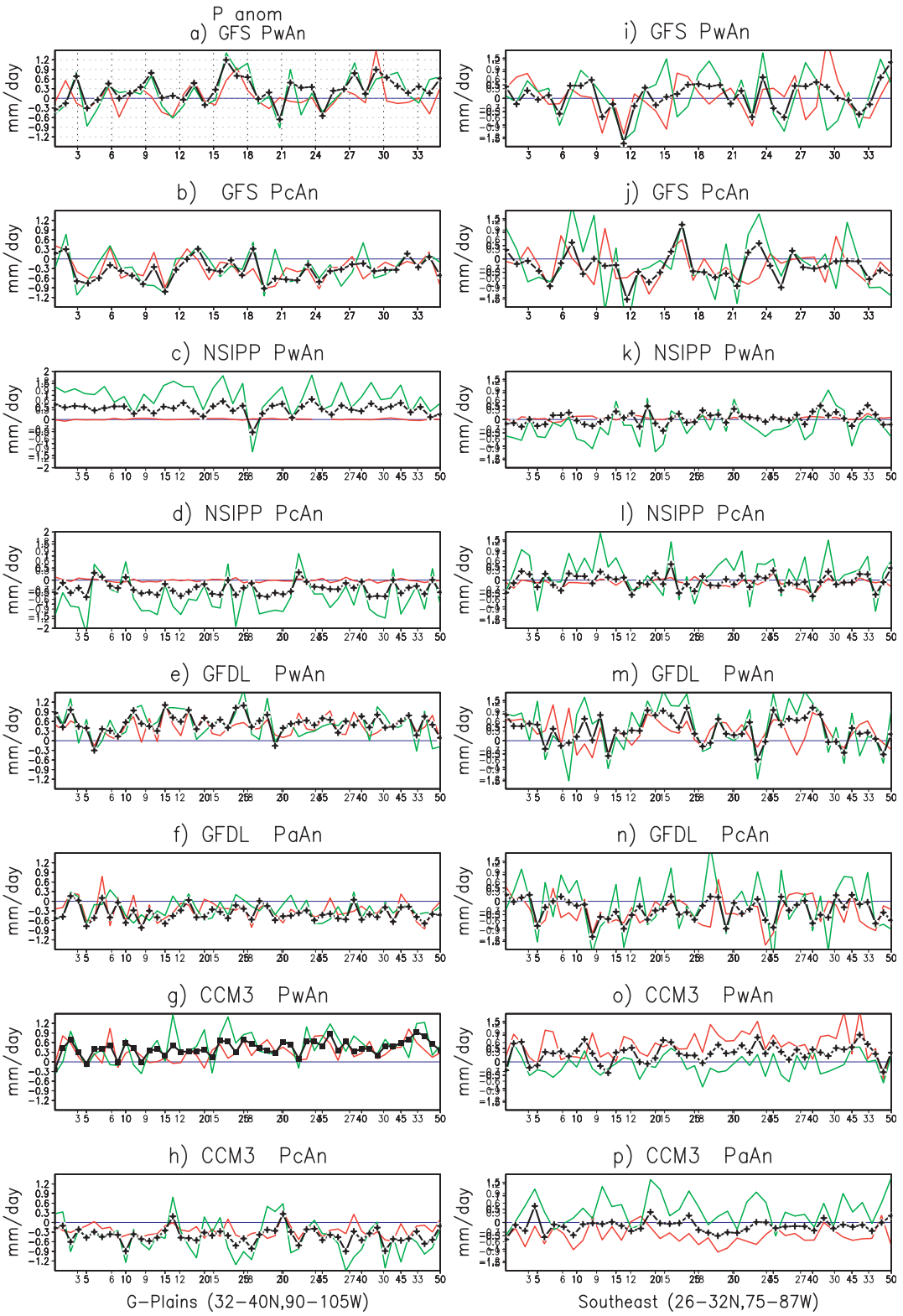

FIG. 5. Mean precipitation anomaly averaged over the Great Plains (32°–40°N, 90°–105°W) for winter (red line), summer (green line), and annual (dark crossed) means for the (a) PwAn GFS, (b) PcAn GFS, (c) PwAn NSIPP, (d) PcAn NSIPP, (e) PwAn GFDL, (f) PcAn GFDL, (g) PwAn CCM3, and (h) PcAn CCM3 experiments. The zero line is marked by the thin blue line. (i)–(p) As in (a)–(h), but for the Southeast (26°–32°N, 75°–87°W over land).

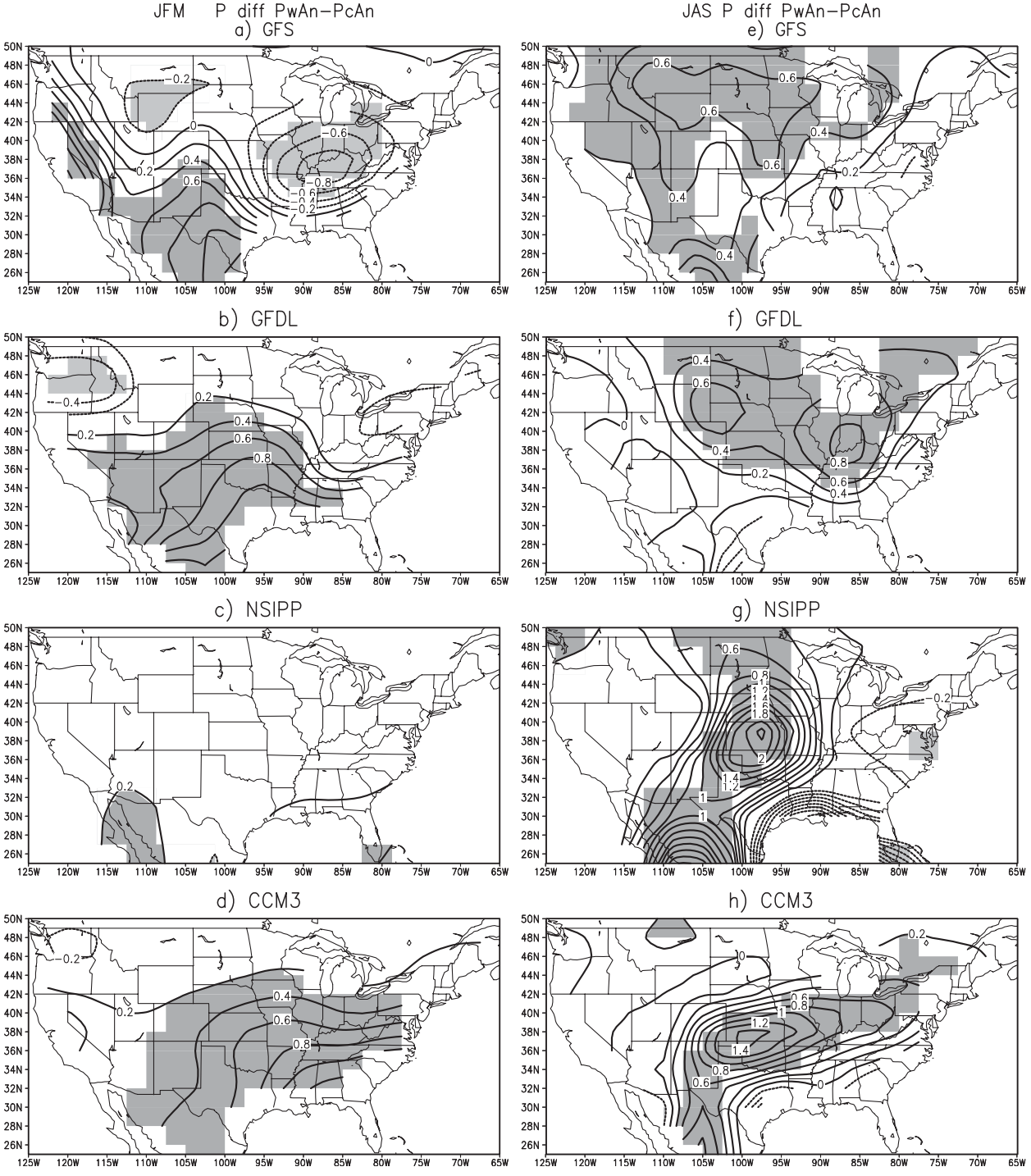

FIG. 6. Mean *P* difference averaged over the last 25 yr of the model integration between PwAn and PcAn for JFM for the (a) GFS, (b) GFDL, (c) NSIPP, and (d) CCM3 experiments. Contour interval is 0.2 mm day^{-1} Areas where positive (negative) anomalies are statistically significant at the 5% level based on the Student's *t* test by assuming 1 degree of freedom yr^{-1} are shaded dark (light). (e)–(h) As in (a)–(d), but for JAS.

too strong. For the CCM3 runs, the response over the western region is too weak and the center of the maximum summer rainfall shifts too far south. The models have large precipitation errors. However, the multimodel ensembles preserve the major responses to the SST forcing. This also confirms the findings of Palmer et al. (2004) and Rowell (1998), which indicate that the multimodel ensemble gives superior results than those of the individual model runs.

Both the model ensembles and composites from the observations indicate that the largest impact of ENSO on drought is over the Southwest, the lower Colorado basin, and the Great Plains, with cold ENSO events favoring droughts. The ENSO influence on drought over the eastern United States, including the East Coast and the Southeast, is limited because the *P* responses to ENSO for winter and summer are opposite in phase.

4. Influence of the Atlantic SSTAs on drought

To study the impact of the Atlantic SSTAs on drought over the United States, the positive and negative cases were selected from the RPC3 associated with the Atlantic pattern (Fig. 1b). The composite difference of SPI6 between positive and negative events averaged over four seasons (Fig. 7b) shows that anomalies are less than 0.8. The influence of the Atlantic SSTAs on drought in the interannual band is small.

To study the decadal influence of the Atlantic forcing, the *P* composite differences between the positive phase (1930–59 and 1995–2006) and negative phase (1915–25 and 1965–90) of the AMO were plotted for winter (Fig. 7a) and summer (Fig. 7d), respectively. These anomalies are statistically significant at only the 10% level and the magnitudes are very weak. There is also no statistically significant signal on the SPI6 composite difference map between warm and cold phase of the AMO averaged over all seasons (Fig. 7e). This suggests that the AMO may create a favorable background state for drought or wet spells to occur, but the direct influence on drought is limited. When data are filtered to focus on the decadal frequency bands, the composites may show a statistically significant signal. Because the percentage of variance contributed by the decadal AMO is small, the total influence on drought from the AMO is weak. This is also confirmed by the model experiments.

The PnAw and PnAc experiments can be interpreted as the atmospheric responses to the decadal warm (PnAw) and cold (PnAc) AMO forcing. The multimodel ensemble frequency of drought occurrence for PnAw and PnAc are given in Figs. 7c,f, respectively. They show that drought is more likely to occur over New Mexico for the warm phase of the AMO. Neither map passes the field significant test. Both model and observational results show that the direct influence of the AMO on drought over the United States is very weak.

5. Modulation of the AMO on the ENSO influence on drought

While the direct impact on drought is small, the AMO can modulate the impact of ENSO or other teleconnections on *P* over the United States (Enfield et al. 2001; Rogers and Coleman 2003). In this section, we examine the modulation of the impact of ENSO on drought by the AMO.

a. Observations

To examine the impact of ENSO and AMO together, ENSO events based on RPC2 were selected for the positive and negative decades of the AMO separately. Composites of SPI6, SRI6, and SM anomalies were computed for each season for cold (warm) ENSO events in the positive decades of the AMO (1930–59 and 1995–2006). Then, we averaged over four seasons. The composites for warm (cold) ENSO events in the negative decades of the AMO (1915–25 and 1965–90) were obtained the same way.

The influence of ENSO on drought is large when the tropical Pacific and the Atlantic SSTAs are opposite in phase (Figs. 8b–e). For the positive AMO and cold ENSO (Figs. 8b–d), drought is favored over the Southwest, the Colorado basin, the Great Plains, the East Coast, and the Southeast. For the negative AMO and warm ENSO (Fig. 8e), wetness is more likely to occur over approximately the same areas except the Southeast where the signal is weak.

When the tropical Pacific and the Atlantic SSTAs are in phase, the net impact on drought is weak (Figs. 8a,f–h). The statistically significant signals are confined to the southern plains and New Mexico, and the magnitudes are small. Overall, results are consistent with Enfield et al. (2001), except that their composites of *P* are limited for winter.

b. Model experiments

The multimodel ensemble means of drought frequencies were presented for experiments with the combined Pacific and Atlantic SSTAs (Fig. 9). They are discussed together with the observational composites (Fig. 8).

Both models and observations indicate that the influence of ENSO on drought over the United States is modulated by the AMO. The influences are greater

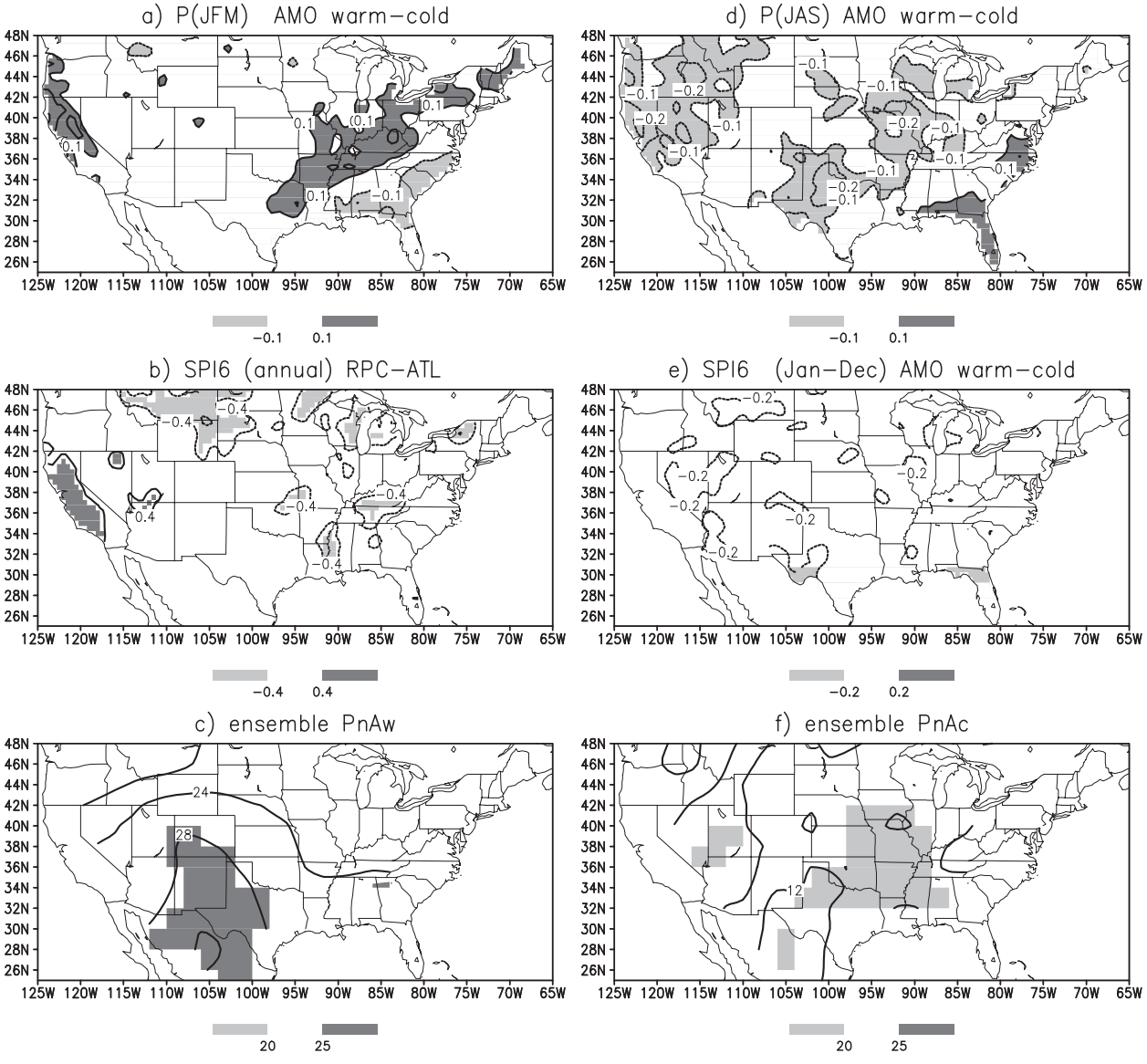

FIG. 7. (a) The *P* anomaly difference between warm and cold decades of the AMO for JFM. Contour interval is 0.1 mm day^{-1}. Positive (negative) anomalies are shaded dark (light). (b) Composite of SPI6 averaged over four seasons based on the RPC associated with Fig. 1b. Contour interval is 0.4. Areas where positive (negative) anomalies are statistically significant at the 5% level based on the Monte Carlo test are shaded dark (light). The *P* anomalies and SPI6 were derived from the *P* analysis. (c) The ensemble mean frequency of drought occurrence × 100 for the model experiment PnAw. Contour interval is 4. Areas where values are statistically significant at the 5% level based on the Monte Carlo test are colored. (d) As in (a), but for JAS; (e) as in (b), but for SPI6 between the warm and cold decades of the AMO. Contour interval is 0.2. (f) As in (c), but for the PnAc experiments.

when the SSTAs in the Pacific and the Atlantic are opposite in phase (PcAw and PwAc). The influence is much weaker when SSTAs in two basins are in phase (PcAc and PwAw).

There is a better chance for drought (wetness) to occur over the Southwest, the Colorado River basin, and the Great Plains for PcAw (PwAc). The areas of the largest uncertainties are located over the East Coast and the Southeast where the model and observations do not agree and the spreads among the models are large (not shown). For example, the model ensemble means for PcAw and PwAc show no signal over the Southeast, but the composites from the observations indicate otherwise.

c. Physical mechanisms

It is difficult to examine the circulation anomalies associated with such modulation based on observations.

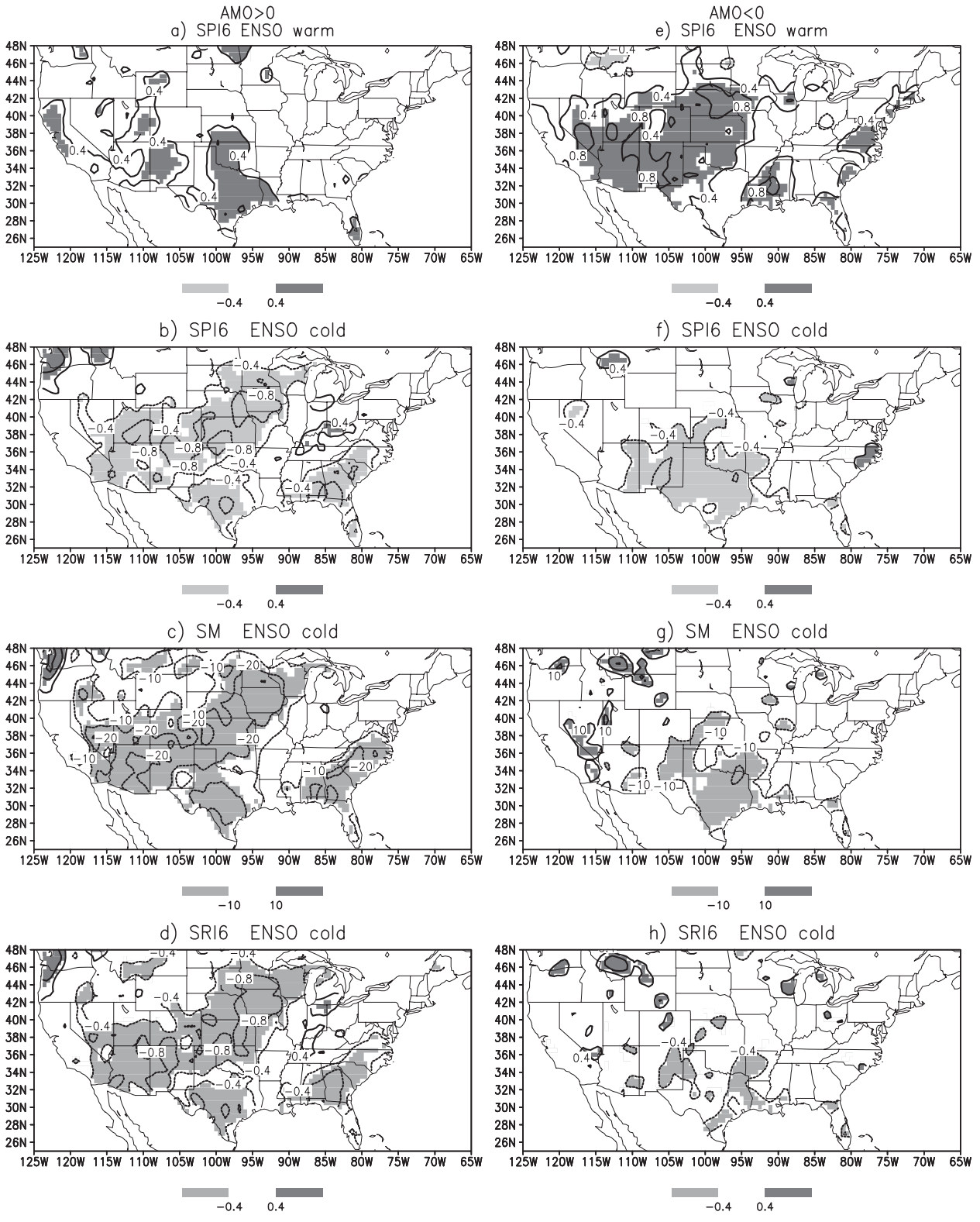

FIG. 8. (a) Composite of SPI6 for warm ENSO based on the RPC associated with Fig. 1a during the positive phase of the AMO. Contour interval is 0.4. Areas where positive (negative) anomalies are statistically significant at the 5% level based on the Monte Carlo test are shaded dark (light). (b) As in (a), but for cold ENSO; (c) as in (b), but for SM anomalies. Contour interval is 10 mm. (d) As in (b), but for SRI6; (e)–(h) as in (a)–(d), but for composites during the negative phase of the AMO.

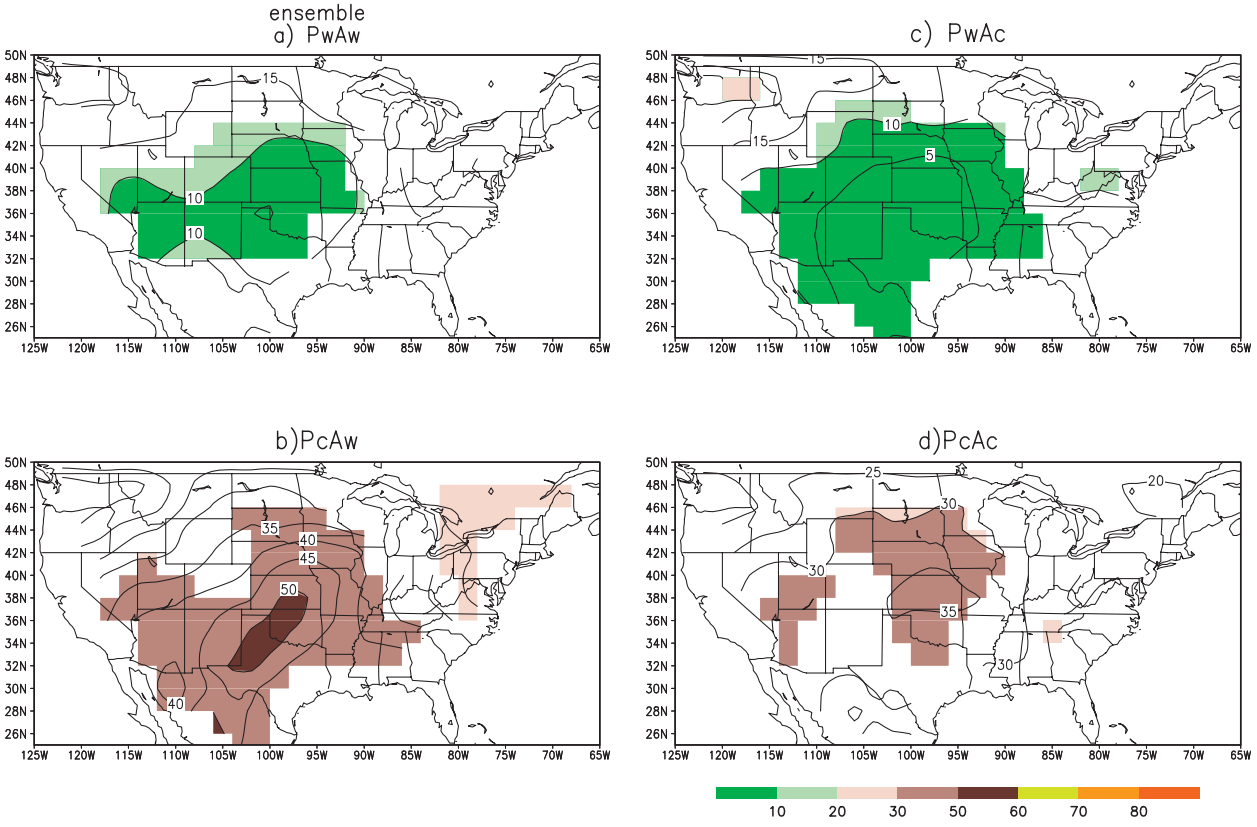

FIG. 9. The ensemble mean frequency of drought occurrence × 100 for the (a) PwAw, (b) PcAw, (c) PwAc, and (d) PcAc experiments. Contour interval is 5. Areas where values are statistically significant at the 5% level based on the Monte Carlo test are shaded.

The NCEP–NCAR reanalysis (Kalnay et al. 1996) starts from 1948 and the dataset is not long enough (one AMO cycle) to obtain robust results. Prior to 1948, there were very limited observations available to obtain reliable objective analysis or data reconstruction. If model simulations are able to capture the signal, then outputs from the model experiments can be used to diagnose the physical mechanisms associated with the indirect influence of the AMO on drought through ENSO.

Because the strongest influence of SSTAs on drought comes from ENSO, we selected models that give realistic *P* responses to ENSO. From *P* anomaly composites (Fig. 6), the model that simulates the realistic winter *P* response to ENSO is the GFS model. All models are able to capture summer (JAS) response over the Great Plains semirealistically. Therefore, the GFS model outputs are used to study the winter case and the ensemble means of four models are used to diagnose the summer case. Discussions are given for the cold ENSO case, but the same mechanisms also work for warm ENSO.

1) WINTER RESPONSES

The major SSTA influence on winter precipitation over the United States comes from ENSO. For cold ENSO, the GFS PcAn experiment captures the precipitation anomaly pattern with dryness over the southern United States and wetness over the Ohio Valley (Fig. 10a). The upper-level jet responds to suppressed convection and shifts northward (colored). The jet extends from the North Pacific (Fig. 10f) to the Southwest. In the tropics, a couplet of negative anomalies (contoured) straddles the equator over the cold SSTAs in the tropical Pacific. In midlatitudes, there is a Pacific–North American type of wave train with positive height anomalies close to the West Coast and negative anomalies to the east. These features are the typical responses to ENSO (Rasmusson and Mo 1993).

The largest responses to the Atlantic SSTAs (PnAc and PnAw) are located in the North Atlantic (Figs. 10g,h), but they are much weaker in comparison to responses to ENSO. The asymmetric responses to warm and cold SSTAs indicate nonlinearity. Features in the North Atlantic can be broadly characterized as a North Atlantic Oscillation (NAO) pattern with positive (negative) phase associated with PnAc (PnAw). As suggested by Peng et al. (2002) and Kushnir et al. (2002), the SSTAs amplify the model's internal variability because the NAO is the leading normal mode. For PnAw, the

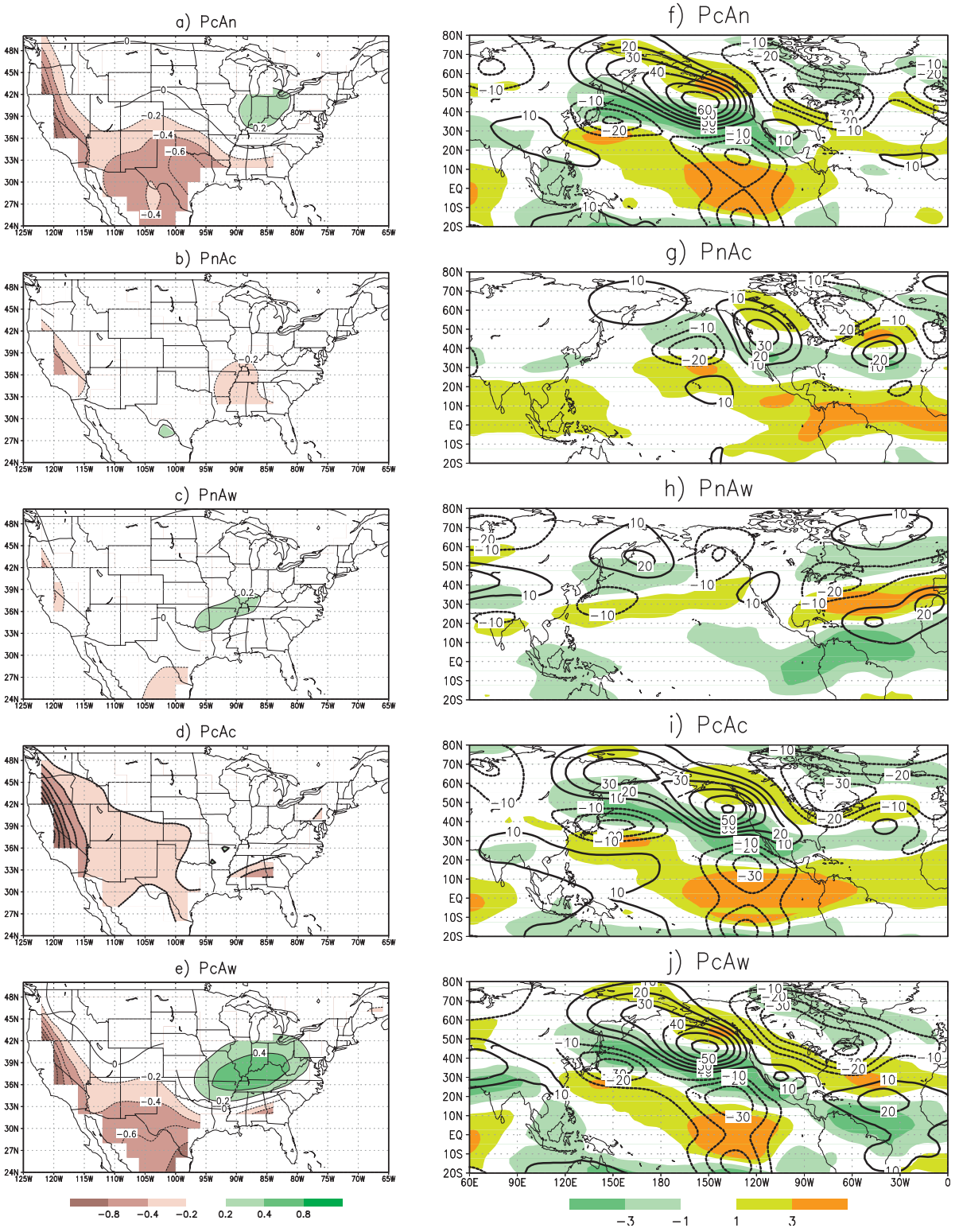

FIG. 10. (a) Composite difference of JFM mean P between the PcAn and PnAn GFS experiments. Contour interval is 0.2 mm day^{-1}. Zero contours are omitted. Areas where values are statistically significant at the 5% level based on the Monte Carlo test are colored. (b) As in (a), but for the PnAc GFS experiment, (c) PnAw GFS experiment, (d) PcAc GFS experiment, and (e) PcAw GFS experiment. (f)–(j) As in (a)–(e), but for the composite of zonal wind U anomalies at 200- (colored) and 200-hPa height anomalies with zonal means removed (contoured). The contour interval is 10 m.

response is more local and confined in the Atlantic, with positive height anomalies over warm water.

For PnAc, the North American jet shifts northward (Fig. 10g). The height anomalies show a wave train with positive height anomalies over the western United States and negative anomalies over the northeastern Canada. For PcAc, with cold SSTAs in both the Pacific and the Atlantic, the height anomalies show the intensification of positive anomalies over the western coast consistent with dryness there (Fig. 10d). The shift of negative anomalies to northern Canada is consistent with diminishing rainfall over the north-central United States.

The 200-hPa height pattern for PnAw shows weak positive anomalies over the western United States and negative anomalies over the Atlantic coast. In comparison to the cold ENSO-only response (Fig. 10f), the response to cold Pacific and warm Atlantic SSTAs (PcAw) shows that the centers of the wave train are shifted (Fig. 10j). Positive anomalies over the West Coast intensify and negative anomalies shift westward. That is consistent with more rainfall over the Ohio Valley and more dryness over the southern United States. For winter, the major influence is ENSO. The presence of SSTAs in the Atlantic (or the AMO) modifies the circulation responses to ENSO over the United States. That in turn modifies the *P* anomalies.

2) SUMMER RESPONSES

For summer, the moisture needed for precipitation over the Great Plains is transported by the Caribbean low-level jet (CALLJ) from the tropical Atlantic to the Gulf of Mexico and by the Great Plains low-level jet (GPLLJ) to the Great Plains (Nunoz et al. 2008; Mo and Berbery 2004). Summer rainfall over the central United States is modulated by the position and the strength of these two low-level jets. The California low-level jet (GCLLJ), which transports moisture from the Gulf of California to the Southwest, influences the North American summer monsoon. Over the East Coast, rainfall is also influenced by tropical storms in the Atlantic. The mean qflux and $D(Q)$ from the GFS are presented in Fig. 11. The climatological mean qflux for JAS indicates that the model captures the CALLJ and the GPLLJ well, albeit the GPLLJ may be too weak (Fig. 11a).

For the cold ENSO SSTAs alone (PcAn), positive 200-hPa height anomalies over the United States (Fig. 12f) are consistent with dryness there (Fig. 12a). The suppressed convection in the tropical Pacific has the downward branch of the anomalous Walker circulation in the Caribbean. Therefore, the CALLJ is weaker (Fig. 11b). The weakening of the GPLLJ is consistent with less rainfall over the northern plains.

The circulation responses to warm and cold SSTAs in the Atlantic are not mirror images of each other. The responses to the Atlantic SSTAs are nonlinear. The PnAw composite (Fig. 12h) shows positive 200-hPa height anomalies over warm SSTAs in the tropical north Atlantic and positive height anomalies over the central-western United States. For moisture fluxes, the anomalous cyclonic circulation in the tropical Atlantic indicates the weakening of the CALLJ associated with the warm SSTAs in the Atlantic and less divergence in the Caribbean (Fig. 11c).

For PcAw (Fig. 12j), positive height anomalies over the central United States are stronger in comparison to the PcAn experiment with cold ENSO alone. That is consistent with more negative rainfall anomalies over the northern plains (Fig. 12e). At the lower level, the moisture flux anomalies show the intensification of the cyclone located in the Atlantic near Florida (Fig. 12e). Both the GPLLJ and the CALLJ are weaker. Less moisture transported into the Great Plains means more divergence or less rainfall (Fig. 12e). For PnAc with cold SSTAs in the Atlantic, there is no statistically significant response in 200-hPa height over the United States (Fig. 12g). The response to PcAc shows the weakening of the positive 200-hPa height anomalies over the central United States (Fig. 12i) and intensification of the anomalous anticyclone over the Atlantic at low levels (Fig. 11f). The overall response is less dryness over the central United States.

6. Conclusions

The influence of ENSO and AMO on drought over the United States is examined using composites from observations and outputs from the model experiments designed by the U.S. CLIVAR drought working group. Experiments were performed by forcing an AGCM with the combinations of the ENSO (Fig. 1a) and/or Atlantic (Fig. 1b) SSTAs superimposed on the monthly mean climatological SSTs (Schubert et al. 2009). The same SSTA forcing repeats each year, so there are no decadal trends involved. There are some limitations of the CLIVAR experiments. For example: these experiments were performed with prescribed SSTAs. The ocean–atmospheric interaction is not included. As demonstrated by Seager et al. (2000), the SSTAs in the Atlantic can be influenced by the atmosphere. The tropical SSTAs over the North Atlantic are likely to be influenced by ENSO (Mo and Hakkinen 2001; Saravanan and Chang 2000, and many others). Therefore, both observations and experiments are utilized to study the influence of SSTAs on drought.

Because drought implies persistent dryness, the 6-month SPI, SRI, and soil moisture anomalies are used to

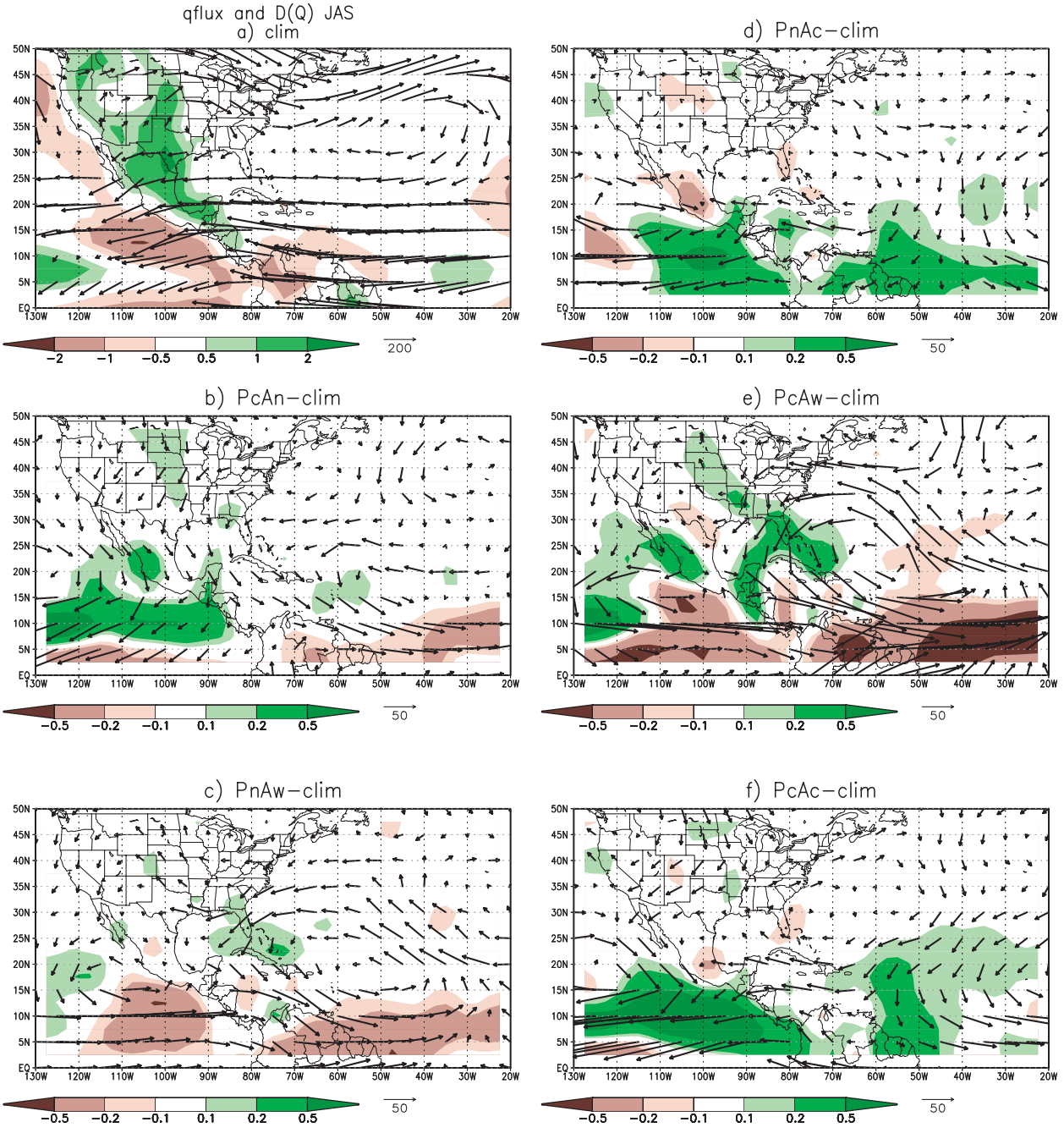

FIG. 11. (a) JAS mean of qflux (vectors) and $D(Q)$ for the GFS PnAn experiment. Areas where $D(Q)$ values are statistically significant at the 5% level based on the Student's t test are colored. The interval is expressed in mm day^{-1}, as indicated by the color bar. The unit vector for the moisture flux is 200 kg m s^{-1}. (b) As in (a), but for the qflux and $D(Q)$ difference for JAS between the PcAn and PnAn experiments. The unit vector is 50 kg m s^{-1}. (c) As in (b), but for the PnAw, (d) PnAc, (e) PcAw, and (f) PcAc experiments.

represent drought. The differences between P and SPI6 composites indicate that persistence is an important condition for drought. Dryness does not imply drought unless it persists for many seasons.

The models respond differently even though they have the same forcing. For each individual model, the simulation of precipitation pattern may or may not be realistic. However, the multimodel ensemble compares favorably with observations. This confirms conclusions in many studies that multimodel ensemble is more reliable than single model results, even for long-term simulations (Palmer et al. 2004; Rowell 1998).

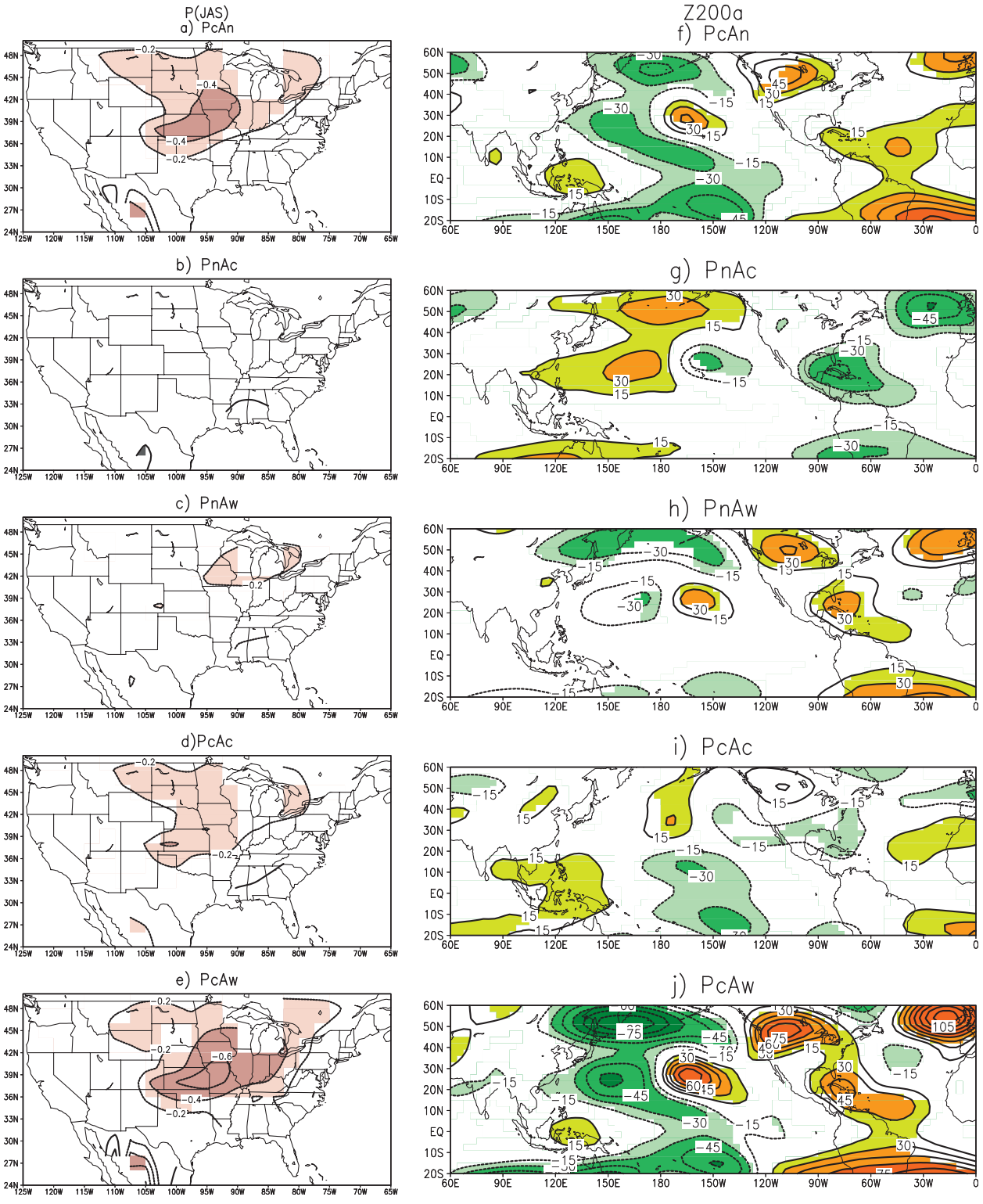

FIG. 12. Composite of JAS *P* mean difference between the ensemble mean PcAn and PnAn experiments. Contour interval 0.2 mm day^{-1}. Zero contours are omitted. Areas where values are statistically significant at the 5% level based on the Monte Carlo test are shaded. (b) As in (a), but for the ensemble PnAc, (c) PnAw, (d) PcAc, and (e) PcAw experiments. (f)–(j) As in (a)–(e) but for the composite of the 200-hPa height anomalies with zonal means removed (contoured). The contour interval is 15 m.

From both model simulations and observations, we conclude the following:

1) The impact of ENSO on drought over the United States is over the Southwest, the Great Plains, and the lower Colorado River basin, with cold ENSO favoring drought. The seasonal cycle over the East Coast and the Southeast is weak. The long-term ENSO impact is small over these areas because the *P* responses to ENSO are opposite in sign for winter and summer. For these areas, a prolonged ENSO lasting two or mode seasons does not always favor a persistent drought or wet spell.
2) The direct influence of the AMO on drought is weak. From observations, the percentage of variance explained by decadal anomalies is small. The composites are not statistically significant. The model experiments (PnAc and PnAw) do not show statistical significant signal. However, the models do show that the atmosphere responds to the Atlantic SSTAs as reported by Kushnir et al. (2002). They suggested that both an eddy-mediated process and the thermodynamic interaction act together to produce a circulation response. Responses for cold and warm SSTAs in the Atlantic are not linear because they are not mirror images of each other. For winter, the circulation response shows a pattern similar to that of the NAO. As suggested by Peng et al. (2002), the model amplifies the model's intrinsic variability. In summer, the Atlantic SSTAs change the strength and location of the Bermuda high and modulate the low-level jet in the Caribbean. However, these responses are not strong enough to influence rainfall.
3) The major influence of the AMO is to modulate the impact of ENSO on drought. The influence on rainfall over the United States is large when the SSTAs in the tropical Pacific and in the North Atlantic are opposite in phase. The cold ENSO in a positive AMO phase favors drought over the Southwest, the Colorado River basin, and the Great Plains. The warm ENSO in a negative AMO phase has the opposite impact. There are large uncertainties of the influence of the AMO and the ENSO over the Southeast and the East Coast. The model simulations have a large spread and do not agree with observations. When the Pacific and the Atlantic SSTAs have the same sign, the influence on rainfall over the United States weakens.

For winter, the Atlantic SSTAs modulate the influence of ENSO by modifying the location of the North American jet and changing the position and strength of anomalies of the wave train. For summer, the GPLLJ already is weakened by cold ENSO event. The warm SSTAs in the Atlantic weaken both the CALLJ and the GPLLJ even more. These low-level jets are responsible for transporting moisture into the Great Plains. The weakening of the low-level jets means less rainfall. The cold Atlantic SSTAs in the warm ENSO phase have the opposite impact.

Our results are consistent with early model simulations (Seager et al. 2005) in which the Pacific SSTAs are the major forcing on droughts or wet spells over the Great Plains and Southwest, with the cold SSTAs in favor of drought. Even though the Atlantic SSTAs play a secondary role, the impact of the SSTAs in the Atlantic cannot be ignored because of its indirect influence.

In addition to SSTAs, soil moisture also plays an important role in maintaining or even strengthening drought. In the Great Plains, the land–atmosphere action is particularly strong (Koster and Suarez 2001; Koster et al. 2005). These are research projects for the future.

Acknowledgments. This work was carried out as a part of a U.S. CLIVAR drought working group activity supported by NASA, NOAA, and NSF to coordinate and compare climate model simulations forced with a common set of idealized SST patterns. The authors thank NASA's Global Modeling and Assimilation Office (GMAO) for making the NSIPP1 runs available, the Lamont-Doherty Earth Observatory of Columbia University for making their CCM3 runs available, NOAA's Climate Prediction Center (CPC) Climate Test Bed (CTB) for making the GFS runs available, NOAA's Geophysical Fluid Dynamics Laboratory (GFDL) for making the AM2.1 runs available, the National Center for Atmospheric Research (NCAR) for making the CAM3.5 runs available, and the Center for Ocean Land Atmosphere (COLA) and the University of Miami's Rosenstiel School of Marine and Atmospheric Science for making the CCSM3.0 coupled model runs available. We wish to thank Dr. Dennis Lettenmainer for providing us the VIC data. This project is supported by the CPPA Grant GC06-012.

REFERENCES

Andreadis, K. M., E. A. Clark, A. W. Wood, A. F. Hamlet, and D. P. Lettenmaier, 2005: Twentieth-century drought in the conterminous United States. *J. Hydrometeor.,* **6,** 985–1001.

Bacmeister, J., P. J. Pegion, S. D. Schubert, and M. J. Suarez, 2000: *An Atlas of Seasonal Means Simulated by the NSIPP 1 Atmospheric GCM*. Vol. 17, NASA Goddard Space Flight Center Tech. Memo. 104606, 194 pp.

Barlow, M., S. Nigam, and E. H. Berbery, 2001: ENSO, Pacific decadal variability, and the U.S. summertime precipitation, drought, and streamflow. *J. Climate,* **14,** 2105–2128.

Campana, K. and P. Caplan, Eds., 2005: Technical procedure bulletin for T382 Global Forecast System. NOAA/NCEP/EMC. [Available online at http://www.emc.ncep.noaa.gov/gc_wmb/Documentation/TPBoct05/T382.TPB.FINAL.htm.]

Dai, A., K. E. Trenberth, and T. R. Karl, 1998: Global variations in droughts and wet spells 1900-1995. *Geophys. Res. Lett.,* **25,** 3367–3370.

——, ——, and T. Quin, 2004: A global dataset of Palmer Drought Severity Index for 1870–2002: Relationship with soil moisture and effects of surface warming. *J. Hydrometeor.,* **5,** 1117–1130.

Delworth, T. L., and Coauthors, 2006: GFDL's CM2 global coupled climate models. Part I: Formulation and simulation characteristics. *J. Climate,* **19,** 643–674.

Enfield, D. B., A. M. Mestas-Nunez, and P. J. Trimble, 2001: The Atlantic Multidecadal Oscillation and its relation to rainfall and river flow over the U.S. *Geophys. Res. Lett.,* **28,** 2077–2080.

Goodrich, G. B., 2007: Influence of the Pacific decadal oscillation on winter precipitation and drought during years of neutral ENSO in the western United States. *Wea. Forecasting,* **22,** 116–124.

Hayes, M. J., M. D. Svoboda, D. A. Wilhite, and O. V. Vanyarkho, 1999: Monitoring the 1996 drought using the standardized precipitation index. *Bull. Amer. Meteor. Soc.,* **80,** 429–438.

Hidalgo, H. G., and J. A. Dracup, 2003: ENSO and PDO effects on hydroclimate variations of the upper Colorado River basin. *J. Hydrometeor.,* **4,** 5–23.

Higgins, R. W., W. Shi, E. Yarosh, and R. Joyce, 2000: *Improved United States Precipitation Quality Control System and Analysis*. NCEP/CPC Atlas No. 7, 40 pp.

Hu, Q., and S. Feng, 2008: Variation of the North American summer monsoon regimes and the Atlantic multidecadal oscillations. *J. Climate,* **21,** 2371–2383.

Kalnay, E., and Coauthors, 1996: The NCEP/NCAR 40-Year Reanalysis Project. *Bull. Amer. Meteor. Soc.,* **77,** 437–471.

Keyantash, J., and J. A. Dracup, 2002: The quantification of drought: An evaluation of drought indices. *Bull. Amer. Meteor. Soc.,* **83,** 1167–1180.

Kiehl, J. T., J. J. Hack, G. Bonan, B. A. Boville, D. Williamson, and P. Rasch, 1998: The National Center for Atmospheric Research Community Climate Model: CCM3. *J. Climate,* **11,** 1131–1149.

Koster, R. D., and M. J. Suarez, 2001: Soil moisture memory in climate models. *J. Hydrometeor.,* **2,** 558–570.

——, and Coauthors, 2005: GLACE: The Global Land–Atmosphere Coupling Experiment. Part I: Overview. *J. Hydrometeor.,* **7,** 590–610.

Kushnir, Y., and I. M. Held, 1996: Equilibrium atmospheric response to North Atlantic SST anomalies. *J. Climate,* **9,** 1208–1220.

——, W. A. Robinson, I. Blade, N. M. J. Hall, S. Peng, and R. Sutton, 2002: Atmospheric GCM response to extratropical SST anomalies: Synthesis and evaluation. *J. Climate,* **15,** 2233–2256.

Maurer, E. P., A. W. Wood, J. C. Adam, D. P. Lettenmaier, and B. Nijssen, 2002: A long-term hydrologically based dataset of land surface fluxes and states for the conterminous United States. *J. Climate,* **15,** 3237–3251.

McCabe, G. J., M. A. Palecki, and J. L. Betancount, 2004: Pacific and Atlantic Ocean influences on multi-decadal drought frequency in the United States. *Proc. Natl. Acad. Sci. USA,* **101,** 4136–4141.

McKee, T. B., N. J. Doesken, and J. Kleist, 1993: The relationship of drought frequency and duration to time scales. Preprints, *Eighth Conf. on Applied Climatology,* Anaheim, CA, Amer. Meteor. Soc., 179–184.

——, ——, and ——, 1995: Drought monitoring with multiple time scales. Preprints, *Ninth Conf. on Applied Climatology,* Dallas, TX, Amer. Meteor. Soc., 233–236.

Mestas-Nunez, A., and D. B. Enfield, 1999: Rotated global modes of non-ENSO sea surface temperature variability. *J. Climate,* **12,** 2734–2746.

Milly, P. C. D., and A. B. Shmakin, 2002: Global modeling of land water and energy balances. Part I: The Land Dynamics (LaD) model. *J. Hydrometeor.,* **3,** 283–299.

Mo, K. C., 2008: Model-based drought indices over the United States. *J. Hydrometeor.,* **9,** 1212–1230.

——, and S. Hakkinen, 2001: Interannual variability in the tropical Atlantic. *J. Climate,* **14,** 2740–2762.

——, and E. H. Berbery, 2004: Low level jets and the summer precipitation regimes over North America. *J. Geophys. Res.,* **109,** D06117, doi:10.1029/2003JD004106.

——, and J. E. Schemm, 2008a: Drought and persistent wet spells over the United States and Mexico. *J. Climate,* **21,** 980–994.

——, and ——, 2008b: Relationships between ENSO and drought over the southeastern United States. *Geophys. Res. Lett.,* **35,** L15701, doi:10.1029/2008GL034656.

Nunoz, E., A. Busalacchi, S. Nigam, and A. Ruiz-Barradas, 2008: Winter and summer structure of the Caribbean low-level jet. *J. Climate,* **21,** 1260–1276.

Palmer, T. N., and Coauthors, 2004: Development of a European Multimodel Ensemble System for Seasonal-Interannual Prediction (DEMETER). *Bull. Amer. Meteor. Soc.,* **85,** 853–872.

Peng, S., A. Mysak, H. Ritchie, J. Derome, and B. Dugas, 1995: The difference between early and middle winter atmospheric response to sea surface temperature anomalies in the northwest Atlantic. *J. Climate,* **8,** 137–157.

——, W. A. Robinson, and S. Li, 2002: North Atlantic SST forcing of the NAO and relationships with intrinsic hemispheric variability. *Geophys. Res. Lett.,* **29,** 1276, doi:10.1029/2001GL014043.

Rasmusson, E. M., and K. C. Mo, 1993: Linkages between 200-mb tropical and extratropical circulation anomalies during the 1986–1989 ENSO cycle. *J. Climate,* **6,** 595–616.

Rogers, J. C., and J. S. M. Coleman, 2003: Interactions between the Atlantic Multidecadal Oscillation, El Niño/La Niña, and the PNA in winter Mississippi Valley stream flow. *Geophys. Res. Lett.,* **30,** 1518, doi:10.1029/2003GL017216.

Ropelewski, C. F., and M. S. Halpert, 1986: North American precipitation and temperature patterns associated with the El Niño/Southern Oscillation. *Mon. Wea. Rev.,* **114,** 2352–2362.

——, and ——, 1989: Precipitation patterns associated with the high index phase of the Southern Oscillation. *J. Climate,* **2,** 268–284.

Rowell, D. P., 1998: Assessing potential seasonal variability with an ensemble of multidecadal GCM simulation. *J. Climate,* **11,** 109–120.

Saha, S., and Coauthors, 2006: The NCEP Climate Forecast System. *J. Climate,* **19,** 3483–3517.

Saravanan, R., and P. Chang, 2000: Interaction between tropical Atlantic variability and El Niño–Southern Oscillation. *J. Climate,* **13,** 2177–2194.

Schubert, S. D., M. J. Suarez, P. J. Pegion, R. D. Koster, and J. T. Bacmeister, 2004: Causes of long-term drought in the U.S. Great Plains. *J. Climate,* **17,** 485–503.

——, and Coauthors, 2009: A U.S. CLIVAR project to assess and compare the responses of global climate models to drought-related SST forcing patterns: Overview and results. *J. Climate,* **22,** 5251–5272.

Seager, R., 2007: The turn of the century North American drought: Global context, dynamics, and past analogs. *J. Climate,* **20,** 5527–5552.

——, Y. Kushnir, M. Visbeck, N. Naik, J. Miller, G. Krahmann, and H. Cullen, 2000: Cause of Atlantic Ocean climate variability between 1958 and 1998. *J. Climate,* **13,** 2845–2862.

——, ——, C. Herweijer, N. Naik, and J. Velez, 2005: Modeling of tropical forcing of persistent droughts and pluvials over western North America: 1856–2000. *J. Climate,* **18,** 4065–4088.

Shukla, S., and A. W. Wood, 2008: Use of a standardized runoff index for characterizing hydrologic drought. *Geophys. Res. Lett.,* **35,** L02405, doi:10.1029/2007GL032487.

Smith, T. M., R. W. Reynolds, R. E. Livezey, and D. C. Stokes, 1996: Reconstruction of historical sea surface temperatures using empirical orthogonal functions. *J. Climate,* **9,** 1403–1420.

Svoboda, M., and Coauthors, 2002: The drought monitor. *Bull. Amer. Meteor. Soc.,* **83,** 1181–1190.

Wang, A., T. J. Bohn, S. P. Mahanama, R. D. Koster, and D. P. Lettenmainer, 2009: Multimodel ensemble reconstruction of drought over the continental United States. *J. Climate,* **22,** 2694–2712.